Cellular Signalling 27 (2015) 2110–2119

Contents lists available at ScienceDirect

Cellular Signalling

journal homepage: www.elsevier.com/locate/cellsig

Elevated IFN-alpha/beta levels in a streptozotocin-induced type I diabetic mouse model promote oxidative stress and mediate depletion of spleen-homing CD8 + T cells by apoptosis through impaired CCL21/CCR7 axis and IL-7/CD127 signaling

Mohamed H. Mahmoud [a,b,1], Gamal Badr [c,*,1], Badr Mohamed Badr [d], Ahmad Usama Kassem [c], Mahmoud Shaaban Mohamed [c]

[a] Deanship of Scientific Research, King Saud University, Riyadh, Saudi Arabia
[b] Food Science and Nutrition Department, National Research Center, Dokki, Cairo, Egypt
[c] Laboratory of Immunology & Molecular Physiology, Zoology Department, Faculty of Science, Assiut University, 71516 Assiut, Egypt
[d] Radiation Biology Department, National Centre for Radiation Research and Technology (NCRRT), Cairo, Egypt

ARTICLE INFO

Article history:
Received 30 May 2015
Received in revised form 27 June 2015
Accepted 1 July 2015
Available online 18 July 2015

Keywords:
Apoptosis
CCL21, CD127, CD8 + T cell
Diabetes
Free radicals
IFN-α/β
Spleen

ABSTRACT

Type 1 diabetes mellitus (T1D) is associated with increased type 1 interferon (IFN) levels and subsequent severe defects in lymphocyte function, which increase susceptibility to infections. The blockade of type 1 IFN receptor 1 (IFNAR1) in non-obese diabetic mice has been shown to delay T1D onset and decrease T1D incidence by enhancing spleen CD4 + T cells and restoring B cell function. However, the effect of type 1 IFN blockade during T1D on splenic CD8 + T cells has not previously been studied. Therefore, we investigated, for the first time, the effect of IFNAR1 blockade on the survival and architecture of spleen-homing CD8 + T cells in a streptozotocin-induced T1D mouse model. Three groups of mice were examined: a non-diabetic control group; a diabetic group; and a diabetic group treated with an anti-IFNAR1 blocking antibody. We observed that T1D induction was accompanied by a marked destruction of β cells followed by a marked reduction in insulin levels and increased IFN-α and IFN-β levels in the diabetic group. The diabetic mice also exhibited many abnormal changes including an elevation in blood and spleen free radical (reactive oxygen species and nitric oxide) and pro-inflammatory cytokine (IL-6 and TNF-α) levels, a significant decrease in IL-7 levels, and subsequently, a significant decrease in the numbers of spleen-homing CD8 + T cells. This decrease in spleen-homing CD8 + T cells resulted from a marked reduction in the CCL21-mediated entry of CD8 + T cells into the spleen and from increased apoptosis due to a marked reduction in IL-7-mediated STAT5 and AKT phosphorylation. Interestingly, type 1 IFN signaling blockade in diabetic mice significantly restored the numbers of splenic CD8 + T cells by restoring free radical, pro-inflammatory cytokine and IL-7 levels. These effects subsequently rescued splenic CD8 + T cells from apoptosis through a mechanism that was dependent upon CCL21- and IL-7-mediated signaling. Our data suggest that type 1 IFN is an essential mediator of pathogenesis in T1D and that this role results from the negative effect of IFN signaling on the survival of splenic CD8 + T cells.

1. Introduction

Type 1 diabetes mellitus (T1D) is a T cell-mediated autoimmune disease that leads to impaired pancreatic insulin-producing β cells [1,2]. Apoptosis has been defined as the main form of β-cell death in the course of insulitis [3]. Insulitis is likely caused by direct contact with activated macrophages and T cells as well as exposure to soluble mediators that are secreted by these cells, including cytokines, nitric oxide (NO) and oxygen free radicals [4]. T helper type 1 (Th1) cells are believed to play a key role in the pathogenesis of T1D in the non-obese diabetic (NOD) mouse, as pancreatic islet-infiltrating mononuclear cells and diabetogenic T cell clones derived from NOD islets show strong Th1 cytokine expression [5–7]. Type I interferons (IFNs), including the α-interferon and β-interferon subtypes, exhibit a vast array of biological functions and strongly affect the immune system [8–10]. One study showed that low IFN-α/β levels are prerequisites for improved IFN-α/β production subsequent to viral infection [11]. Additionally, elevated type I IFN levels during T1D suggested lymphocyte exhaustion and a defective lymphocyte-medicated immune response [12]. Moreover, type I IFN overexpression during diabetes could be a

* Corresponding author at: Zoology Department, Faculty of Science, Assiut University, 71516 Assiut, Egypt.
E-mail addresses: badr73@yahoo.com, gamal.badr@aun.edu.eg (G. Badr).
URL: http://www.aun.edu.eg/ (G. Badr).
[1] These authors are co-first authors.

http://dx.doi.org/10.1016/j.cellsig.2015.07.005
0898-6568/

major cause of impaired lymphocyte immune responses [13,14]. In addition, previous studies have determined the involvement of IFN-α in T1D development, as elevated IFN-α mRNA and protein levels can be detected in the pancreata of T1D patients compared with non-diabetic patients [15].

Oxidative stress has been implicated in the development of diabetic complications [16]. Reactive oxygen and nitrogen species (ROS/RNS) participate in T1D development and progression through glucose autoxidation, protein glycation, NADPH consumption through the polyol pathway, and protein kinase C activation [14–19]. Furthermore, diabetes induction leads to high production levels of ROS, hydroperoxide, malondialdehyde (MDA), and proinflammatory cytokines, including IL-1α, IL-1β, IL-6, and CXCL10 [18,19]. However, the main cytokines involved in diabetes pathogenesis are IL-1, TNF-α, and IL-6 [20].

Mature lymphocytes, which differentiate in primary lymphoid organs, are released into the peripheral blood and circulate to the secondary lymphoid organs, where they respond to antigens [21]. Furthermore, infiltrating CD8+ T cells have been shown to have exclusive specificity towards islet auto-antigens, which emphasizes their autoreactive nature and classifies T1D among the prototype tissue-specific autoimmune diseases [22]. Moreover, it is well established that CD8+ T cells play essential roles in the early events leading to insulitis and in diabetes in NOD mice [23,24]. Although the role of T cells as effectors of β-cell destruction in diabetes is well established, the nature of the antigens, cells, and the mechanisms that prime diabetogenesis remain poorly understood [25].

Previous studies have demonstrated the essential role of chemokines and chemokine receptors in leukocyte trafficking and homing to lymphoid tissues that are thought to be important in immune responses [21,26]. The entry of T lymphocytes into lymph nodes (LNs) and their homing to the secondary lymphoid organ T cell zones, such as in the spleen, are controlled by CC chemokine receptor 7 (CCR7) and its ligands, CCL19 and CCL21 [27–29]. Additionally, CCR7 and its ligands (CCL19 and CCL21) may be involved in the development and/or progression of islet inflammation, β-cell destruction and T1D [30]. The different homing patterns of naive and effector CD8 T cells in vivo correlated well with their CCR7 chemokine receptor expression and their reactivity to secondary lymphoid tissue chemokine (SLC). Hence, CCR7 expression down-regulation on CD8 effector T cells made them unresponsive to SLC, which controls T cell homing into splenic and lymph node white pulp [31].

IL-7 plays a pivotal role in naïve and memory CD8+ T cells by stimulating thymopoiesis and controlling peripheral T lymphocyte homeostasis [32–37]. Moreover, IL-7 suppressed programmed cell death protein 1 (PD-1) expression after T cell activation, and IL-7 can promote IFN-γ+ cell development in CD4+ and CD8+ T cells, both T cell subsets of which contribute to T1D pathogenesis [38]. We recently demonstrated that blocking type 1 IFN during diabetes rescues B lymphocytes from apoptosis [14]. However, in the present study, we focused on the effect of type 1 IFN receptor blockade on spleen-homing CD8+ T cells.

2. Materials and methods

2.1. Chemicals

Streptozotocin (STZ) was obtained from Sigma Chemicals Co. (St. Louis, MO, USA) and dissolved in cold 0.01 M citrate buffer (pH 4.50) immediately before use (within 5 min).

2.2. Animals and experimental design

Laboratory BALB/c mice weighing 25–30 g were obtained from Theodor Bilharz Research Institute, Cairo, Egypt. All animal procedures were performed in accordance Declaration of Helsinki with the guidelines for the care and use of experimental animals that was established by the Committee for the Purpose of Control and Supervision of Experiments on Animals (CPCSEA) and the National Institute of Health (NIH) protocol. The animals were allowed to acclimate for 2 weeks before the experiments and were housed in metal cages in a well-ventilated room. The animals were maintained under standard laboratory conditions (25 °C, 60–70% relative humidity and a 12-hour light/dark cycle) and were fed a standard commercial pellet diet and water. Forty five BALB/c mice were assigned to 3 experimental groups: group 1, the non-diabetic control group (n = 15), which was injected with vehicle alone (0.01 M citrate buffer, pH 4.5); group 2, the diabetic group (n = 15), which was rendered diabetic by five consecutive intraperitoneal injection STZ doses (60 mg per kilogram of body weight/day for five days) in 0.01 M citrate buffer (pH 4.5); group 3 (n = 15) was rendered diabetic using the same procedure as in group 2 but was also injected intraperitoneally, 1 month after diabetes induction, with an anti-IFNAR1 antibody at a dose of 10 mg per kilogram of body weight daily for up to 20 days, as previously described [39].

2.3. Blood samples

At the end of the experiment (after treatment with anti-IFNAR1 for 21 days), the mice were anesthetized with pentobarbital (60 mg per kilogram of body weight), the abdominal cavity was opened, and whole blood was drawn from the abdominal aorta. Plasma was obtained by low-speed centrifugation (1000 ×*g* for 20 min) and immediately stored at −80 °C for further insulin measurement. PBMCs were isolated from heparinized blood using the Ficoll gradient method.

2.4. Insulin level measurement

Plasma insulin levels were determined with commercially available enzyme-linked immunosorbent assay (ELISA) kits (R&D Systems, USA) according to the manufacturer's instructions. The insulin concentration was then calculated using a standard insulin curve, which was included on the same plate as the samples.

2.5. Cytokine measurements

The levels of plasma cytokine IL-6, IL-7, TNF-α, IFN-α and IFN-β were determined with commercially available ELISA kits (R&D Systems, USA), as previously described [40] according to the manufacturer's instructions. The cytokine concentrations were then calculated using a standard cytokine curve, which was included on the same plate as the samples.

2.6. ROS and NO level measurements

ROS levels were measured with 2,7-dichlorodihydrofluorescein diacetate (H2DCF-DA; Sigma-Aldrich). The samples were directly treated with 10 μM H2DCF-DA that was dissolved in 1 ml of phosphate buffer saline (PBS) at 37 °C for 20 min. The fluorescence intensity was monitored with an excitation wavelength of 488 nm and an emission wavelength of 530 nm. The nitrite and nitrate concentrations were measured with a Griess reagent assay kit (NO_2/NO_3 detection kit; Dojindo, Kumamoto, Japan) according to the manufacturer's instructions. In brief, the azo coupling between the diazonium species (which are produced from a reaction between sulfanilamide and NO_2) and N-(1-naphthyl) ethylenediamine was measured at 540 nm with an MRX microplate reader (Dynex Technologies, Inc., Chantilly, VA, USA).

2.7. Histology and immunohistochemistry

Spleen tissues were fixed overnight in a freshly prepared 4% paraformaldehyde solution in 0.1 M PBS, pH 7.4, at 4 °C. The samples were dehydrated and prepared as paraffin blocks. We used an anti-CD8 (1:100; Abcam) primary monoclonal antibody to detect and monitor

the spleen-homing CD8 + T cells in the spleen sections. The appropriate primary antibody was added in the blocking buffer and incubated overnight at 4 °C. The sections were washed and incubated with a biotinylated secondary antibody at a 1:2000 dilution for 2 h at room temperature, followed by washing and incubation with an avidin–biotin complex (VECTASTAIN Elite ABC kit; Vector Laboratories, Burlingame, CA, USA) at a 1:100 dilution for 1 h at room temperature. The sections were counterstained with Mayer hematoxylin for 2 to 5 min and mounted.

2.8. Electron microscopic examinations

For the electron microscopic examination, small spleen pieces (1 × 1 mm) from the three animal groups were quickly removed and fixed in 5% cold glutaraldehyde buffer for one week. The specimens were then washed with PBS (pH 7.2) for 15 min 4 times with slow shaking and post fixed in 1% osmium tetroxide for 2 h. The slides were washed again with PBS and then dehydrated using the following ascending alcohol grades: 50% for 30 min; 70% overnight; 95% for 30 min; and finally, with 3 30-minute 100% washes. The samples were embedded in propylene oxide for 30 min to remove any alcohol remnants. Then, the samples were embedded in propylene oxide plus Epon 812 (1:1, v/v) for 30 min and were then embedded in Epon 812 for 4 h. The samples were finally embedded into capsules containing the embedding mixture, and the tissue blocks were polymerized in an oven for 2 days at 60 °C. Semi-thin 0.5-μm sections were prepared with an LKB ultra microtome and then stained with toluidine blue. The semi-thin sections were examined for localization of the desired tissues, and then, ultrathin sections were prepared, accordingly. The sections were stained with uranyl acetate and lead citrate and examined with a transmission electron microscope (Jeol, 100 CXII), which was operated at 80 kV in the Electron Microscopic Center, Assiut University. Electron micrographs were captured for the selected semi-thin regions, reconstructed and processed using Photoshop software to examine the spleens from each group.

2.9. Isolation of the splenic lymphoid cell population

The spleens were washed with sterile PBS twice and put on petri dishes containing sterile PBS. The spleens were then pressed with a syringe. The subsequent single cell solutions were filtered with a sterile wire and put into 15-ml polypropylene tubes. Next, PBS was added to the cell suspensions in the polypropylene tubes to a final volume of 10 ml and then centrifuged for 5 min (2500 rpm, at 4 °C). Then, the supernatant was discarded, and the obtained pellet was resuspended with 1 ml of sterile PBS. Single cell suspensions containing 2×10^6 cells were washed and cultured for 4 h in RPMI complete culture media prior to staining for flow cytometry and Western blot analyses.

2.10. Flow cytometry analysis

Cell surface antigen expression was determined with single-parameter fluorescence-activated cell sorter (FACS) analysis using the following monoclonal antibodies (mAbs) purchased from BD Biosciences: PE-conjugated anti-CD8; FITC-conjugated anti-CCR7 and anti-CD127; FITC-conjugated Annexin V; and FITC- and PE-conjugated mouse isotype-matched control mAbs. Following the 4-hour culture incubation, splenic lymphocytes were washed 3 times in PBS followed by 2 washes with FACS buffer (1% BSA in PBS) and double stained with PE-conjugated anti-CD8 and FITC-conjugated CCR7, CD127 or IgG2a isotype control (10 μl antibody/10^6 cells) at 4 °C for 30 min. The cells were then washed with FACS buffer, resuspended and stored in 500 μl of 2% paraformaldehyde solution. A FACSCalibur flow cytometry instrument (BD-PharMingen) was used for the data acquisition and analysis. After viable cell gating, 15,000 events per sample were analyzed. For each marker, the positivity threshold was defined beyond the non-specific binding that was observed in the presence of a relevant isotype control mAb.

2.11. Mitochondrial membrane potential measurements

The mitochondrial energy status was determined by examining the cellular retention of a JC-1 dye (Molecular Probes), as previously described [41]. The membrane-permeable JC-1 dye is widely used in apoptosis studies to monitor mitochondrial health and can be used as a mitochondrial membrane potential indicator in a variety of cell types. The JC-1 dye exhibits potential-dependent accumulation in mitochondria, which is indicated by a fluorescence emission shift from green (~529 nm) to red (~590 nm). Consequently, mitochondrial depolarization is indicated by a decrease in the red/green fluorescence intensity ratio. The potential-sensitive color shift is due to concentration-dependent formation of red fluorescent J-aggregates. Briefly, splenic lymphocytes (5×10^5) were loaded with JC-1 dye (1 μg/ml) for 30 min at 37 °C in a 5% CO_2 incubator. The cells were then washed twice with PBS, washed once with FACS buffer, resuspended and then stored in 500 μl of 2% paraformaldehyde solution. Approximately 10^5 cells were analyzed with flow cytometry. Fluorescence was monitored in a fluorometer at 570 nm excitation/595 nm emission wavelengths for the J-aggregate of JC-1 examination. The mitochondrial membrane potential ($\Delta\psi_m$) was calculated as a ratio of the JC-aggregate (aqueous phase) fluorescence to the monomeric JC-1-form fluorescence (membrane-bound). This process allowed for discrimination between the apoptotic (green) and healthy (red) cells.

2.12. In vitro chemotaxis assays

The chemokine-dependent migration of splenic lymphocytes was measured with an in vitro 2-chamber migration assay (using Transwell plates that were purchased from Costar, Cambridge, MA, USA) followed by flow cytometry analysis. All chemotaxis assays were performed in pre-warmed migration buffer (RPMI 1640 containing 1% FCS). A total of 600 μl of migration buffer alone or buffer that was supplemented with CCL21 (at 250 ng/ml; R&D Systems) was added to the lower chamber, and 10^5 cells in migration buffer were added to the upper chamber. The plates were then incubated for 3 h at 37 °C; the input and transmigrated cells were centrifuged and then stained with PE-conjugated anti-CD8 mAb for 30 min. The cells were then washed, fixed in 300 μl of 1× PBS + 1% formaldehyde and counted for 60 s via flow cytometry. The migration percentage was calculated as the percentage of input CD8 + T cells that migrated to the lower chamber. To calculate the percentage of the CCL21-mediated specific migration, the percentage of CD8 + T cells that migrated to medium alone was subtracted from the percentage of CD8 + T cells that migrated to the medium with chemokine.

2.13. Western blot analysis

Prior to Western blot analysis, 5×10^6 CD8 + population cells, which were isolated with magnetic beats from spleen tissues from five animals per group, were incubated in pre-warmed RPMI-1640 without FCS and were stimulated or not with IL-7 for 5 min. Lysates were then prepared as previously described [42], and equal amounts of the total cellular protein were subjected to SDS-PAGE and blotted onto a nitrocellulose membrane (Millipore, Bedford, MA, USA). After primary antibodies recognizing phospho-STAT5, total-STAT5, phospho-AKT, and total-AKT (Cell Signaling, UK) were diluted 1:500 in 1× Tris buffer saline (TBS) with 0.1% Tween-20 and 5% bovine serum albumin (BSA), the membrane was incubated overnight with a primary antibody on an orbital shaker at 4 °C. Following the overnight incubation, the primary antibody was removed, and the membrane was washed three times in washing buffer for 5 min. A horseradish peroxidase (HRP)-labeled goat anti-mouse gamma globulin secondary antibody (Cell Signaling, UK) was

diluted to 1:1000 and applied to the membrane for 1 h at room temperature on an orbital shaker. The membrane was then washed three times in washing buffer for 5 min, followed by a single wash in distilled water for 5 min. The antigens were visualized with a chemiluminescence substrate (ECL, SuperSignal West Pico Chemiluminescent Substrate; Perbio, Bezons, France) and exposure to X-ray film (Amersham Biosciences, France). The ECL signal was specifically recorded on ECL hyper-film. To quantify the band intensities, the films were scanned, saved as TIFF files and analyzed with the NIH ImageJ software.

2.14. Statistical analyses

The data were tested for normality with the Anderson–Darling test and for homogeneity variances prior to further statistical analysis. The data were normally distributed and are expressed as the mean ± standard error of the mean (SEM). Significant differences among the groups were analyzed with one- or two-way ANOVA tests followed by the Bonferroni's test for multiple comparisons with the PRISM statistical software (GraphPad Software). The data were also reanalyzed with one- or two-way ANOVA tests followed by the Tukey's post-test with the SPSS software, version 17. Differences were considered significant at $P < 0.05$. *$P < 0.05$ for diabetic versus control; #$P < 0.05$ for diabetic + anti-IFNAR1 antibody versus diabetic; +$P < 0.05$ for diabetic + anti-IFNAR1 versus control.

3. Results

3.1. T1D induction is accompanied by a marked elevation in IFN-α and IFN-β levels

To optimize the parameters and conditions of the animal models during experimentation, the blood glucose and insulin levels of the three mouse groups (n = 10) were monitored after diabetes induction (Table 1). The glucose levels in both the diabetic and type I IFN signaling-blocked diabetic groups were significantly higher than those in the control normal non-diabetic group. By contrast, the insulin levels were significantly decreased in the diabetic and type I IFN signaling-blocked diabetic groups compared with the non-diabetic control group. Interestingly, the diabetic mice exhibited an obvious and significant increase in the IFN-α and IFN-β levels compared with the control non-diabetic mice. Blocking type I IFN receptor in diabetic mice partially but not significantly restored the altered IFN-α and IFN-β levels compared with the diabetic non-treated mice.

3.2. IFNAR1 blockade restores free radical, pro-inflammatory cytokine and IL-7 levels in diabetic mice

We monitored the oxidative stress levels in the blood and the spleen of the three mouse groups. The data acquired for ten individual mice per group are shown (Fig. 1A). In the diabetic mice (gray, filled bars), we observed aberrant and significantly increased ROS and NO levels compared with the control non-diabetic group (black, filled bars).

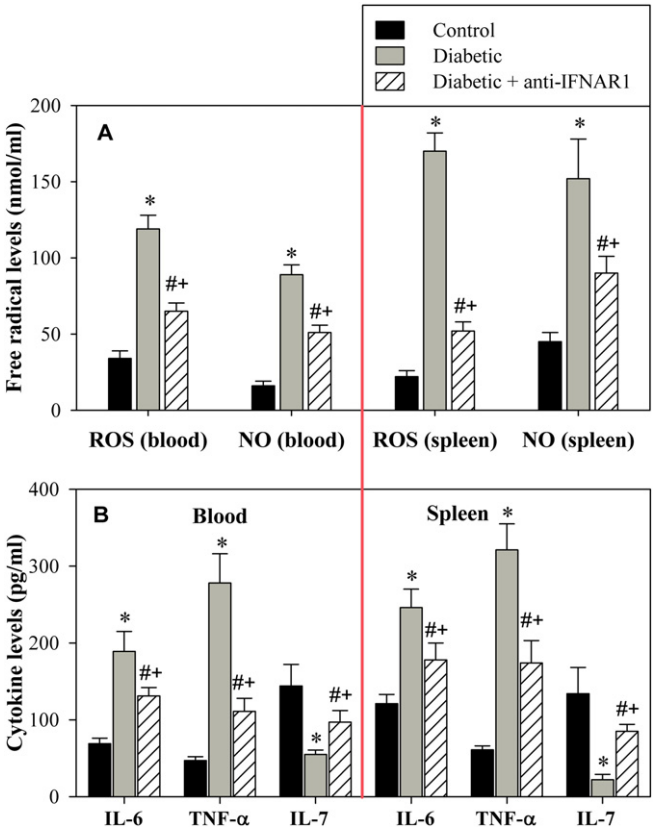

Fig. 1. Diabetes induction elevates levels of oxidative stress and alters TNF-α, IL-6 and IL-7 levels. (A) The oxidative stress biochemical parameters, ROS and NO, were measured in the blood and the spleen in the three mouse groups, and the results are presented as the mean ± SEM (n = 10). (B) Blood and spleen cytokine levels (TNF-α, IL-6 and IL-7) were measured in the three mouse groups with ELISAs. The results are presented as the mean ± SEM (n = 10); *$P < 0.05$, diabetic vs. control; +$P < 0.05$, diabetic + anti-IFNAR1 vs. control; #$P < 0.05$, diabetic + anti-IFNAR1 vs. diabetic.

Interestingly, type I IFN signaling blockade in the diabetic mice (hatched bars) significantly decreased ROS and NO levels in both the blood and spleen compared with the diabetic non-treated mice. Furthermore, we monitored the blood and splenic TNF-α, IL-6 and IL-7 cytokine levels, which can alter immune cell function during diabetes in the three mouse groups. The data acquired for ten individual mice per group revealed that the diabetic mice exhibited significantly elevated IL-6 and TNF-α level in both the blood and spleen compared with the control group, which indicated prolonged pro-inflammatory conditions during diabetes (Fig. 1B). By contrast, the blood and splenic IL-7 levels were significantly decreased in the diabetic mice compared with the control group.

3.3. IFNAR1 blockade in diabetic mice restores the number and distribution of CD8 + T cells in the spleen

To investigate the spleen-homing CD8 + T cell architecture during T1D, immunohistochemical techniques were applied to paraffin sections in the white (Fig. 2A) and red pulp (Fig. 2B) of the spleens of the three mouse groups. Accumulated data from three animals per group are presented. In the control animals, large CD8 + T cell numbers were present in the periarterial lymphatic sheath (PALS), and moderate numbers of these cells were present in the germinal center of the lymphatic nodules and the red pulp. Moreover, an obvious decrease in the number of CD8 + T cells in the red pulp of the spleens, the marginal zone of the white pulp and in the lymph follicles were observed in the diabetic group compared with the control group. Interestingly, IFNAR1 blockade in the diabetic mice clearly returned the CD8 + T cell numbers

Table 1
Glucose, insulin, IFN-α and IFN-β levels were altered during diabetes. Blood glucose, insulin, IFN-α and IFN-β levels were monitored in the 3 mouse groups. Accumulated data from 10 separate individual mice from each group are shown. The data were first tested for normality and variance homogeneity prior to any further statistical analysis. The data were normally distributed and are expressed as the mean ± SEM. *$P < 0.05$, diabetic vs. control; +$P < 0.05$, diabetic + anti-IFNAR1 vs. control; #$P < 0.05$, diabetic + anti-IFNAR1 vs. diabetic (ANOVA with Tukey's post-test).

Parameters	Control group	Diabetic group	Diabetic + anti-IFNAR1 group
Glucose (mg/dl)	112 ± 10.4	396 ± 32*	313 ± 28$^{\#,+}$
Insulin (ng/ml)	5.8 ± 0.8	1.4 ± 0.4*	2.9 ± 0.54$^{\#,+}$
IFN-α (ng/ml)	1.2 ± 0.28	5.8 ± 0.6*	4.8 ± 0.38^{+}
IFN-β (ng/ml)	1.8 ± 0.16	4.9 ± 0.42*	4.4 ± 0.3^{+}

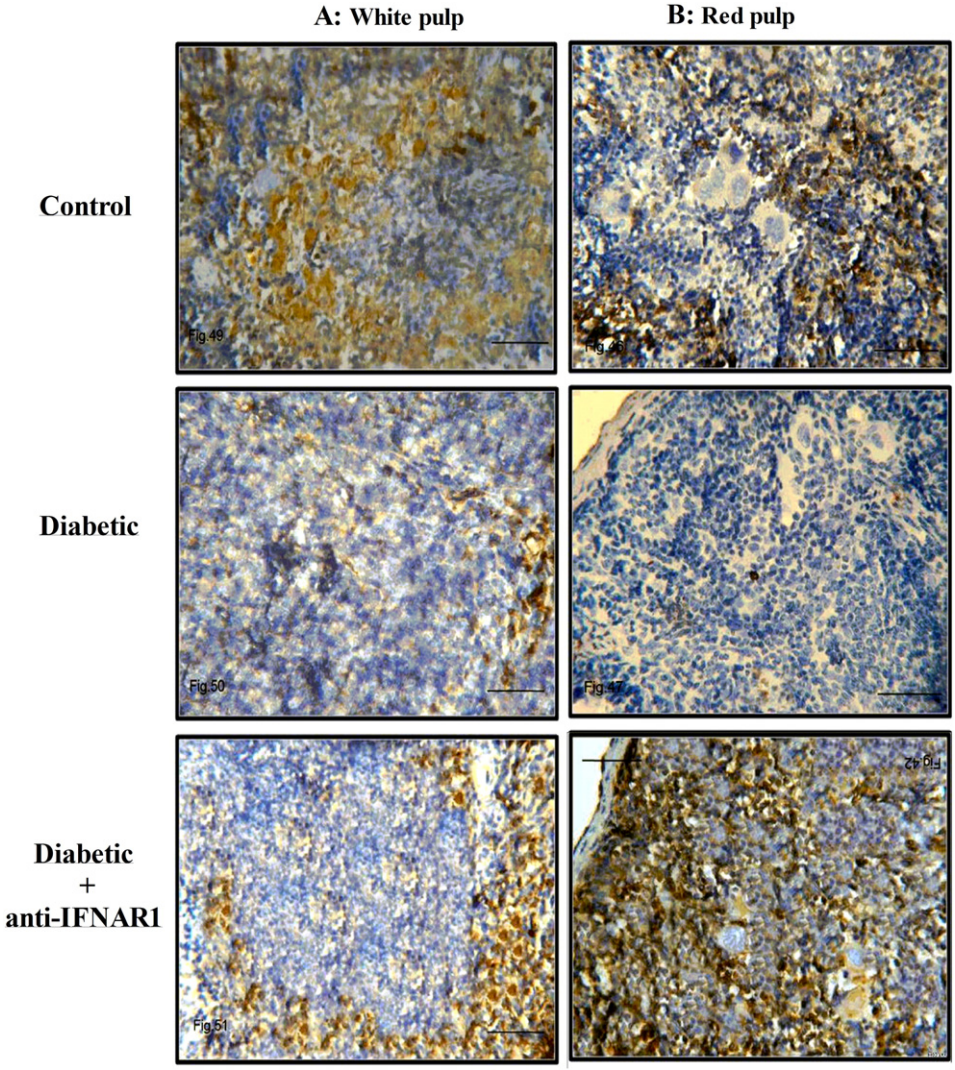

Fig. 2. Altered CD8 + T cell numbers and distribution in the spleens of diabetic mice. CD8 + T cells in the mouse spleen white pulp (A) and red pulp (B) were detected by immunohistochemical analysis (immunoperoxidase 40×). Numerous CD8 + T cells (brown-colored cells) were normally distributed in the marginal zone of the white pulp, the germinal center of the lymphatic follicles and the red pulp in the control mice. One representative experiment out of three is shown.

to their normal levels in the red pulp, marginal zone and in the PALS of white pulp compared with the diabetic group.

3.4. IFNAR1 blockade in diabetic mice rescues spleen CD8 + T cells from apoptosis induced by mitochondrial membrane potential alterations

To investigate the protective effect of IFNAR1 blockade on CD8 + T cell survival during diabetes, isolated splenic T cells were double stained with a PE-conjugated anti-CD8 and FITC-conjugated Annexin V as indicator of early apoptosis and were then analyzed by flow cytometry. As shown in one representative experiment with control mice (gray, filled histogram), diabetic mice (red, filled histogram) and diabetic mice treated with anti-IFNAR1Ab (blue, filled histogram), the CD8 + T cell percentage within T cell population that underwent early apoptosis was increased in the diabetic group compared with the control group (Fig. 3A). By contrast, type I IFN blockade significantly reduced the early apoptotic CD8 + T cell percentage. The mitochondrial membrane plays a pivotal role in determining cell survival or death. Therefore, we monitored the mitochondrial membrane potential of CD8 + T cells with JC-1 dye followed by flow cytometry analysis. One representative experiment with control mice, diabetic mice and diabetic mice treated with anti-IFNAR1 Ab demonstrates the distinct clustering of viable (red) and apoptotic (green) cells that was observed. The cell shift from the upper panel (red dots) to the lower panel (green dots) indicates a decrease in the mitochondrial membrane potential and a subsequent increase in apoptosis induction in the CD8 + T cells from the diabetic mouse (67%) compared with the control non-diabetic mouse (7%). In this context, the anti-IFNAR1 Ab treatment clearly decreased the apoptosis induction in the diabetic cells from 67% to 29%, compared with 7% in the control group (Fig. 3B). The pooled data from ten individual mice from each group indicated that anti-IFNAR1 treatment of the diabetic mice (hatched bars) significantly restored the mitochondrial membrane potential alterations of the diabetic non-treated mouse spleen CD8 + T cells (gray, filled bars) and therefore decreased both early and late apoptosis of CD8 + T cells during diabetes compared with control non-diabetic mice (black, filled bars; Fig. 3C). Interestingly, ultra-sections of the control mouse spleens showed that the mature and immature granulocytes and lymphocytes were healthy; however, the diabetic mouse spleen sections showed several apoptosis-related changes, as the lymphocytes exhibited nucleus indentation and swollen mitochondria with disorientated and disintegrated cristae, as well as plasma cells that exhibited karyolysis of the nucleus and dilated extensive rough endoplasmic reticulum. One representative experiment out of three per group is shown (Fig. 3D). Furthermore, blocking IFNAR1

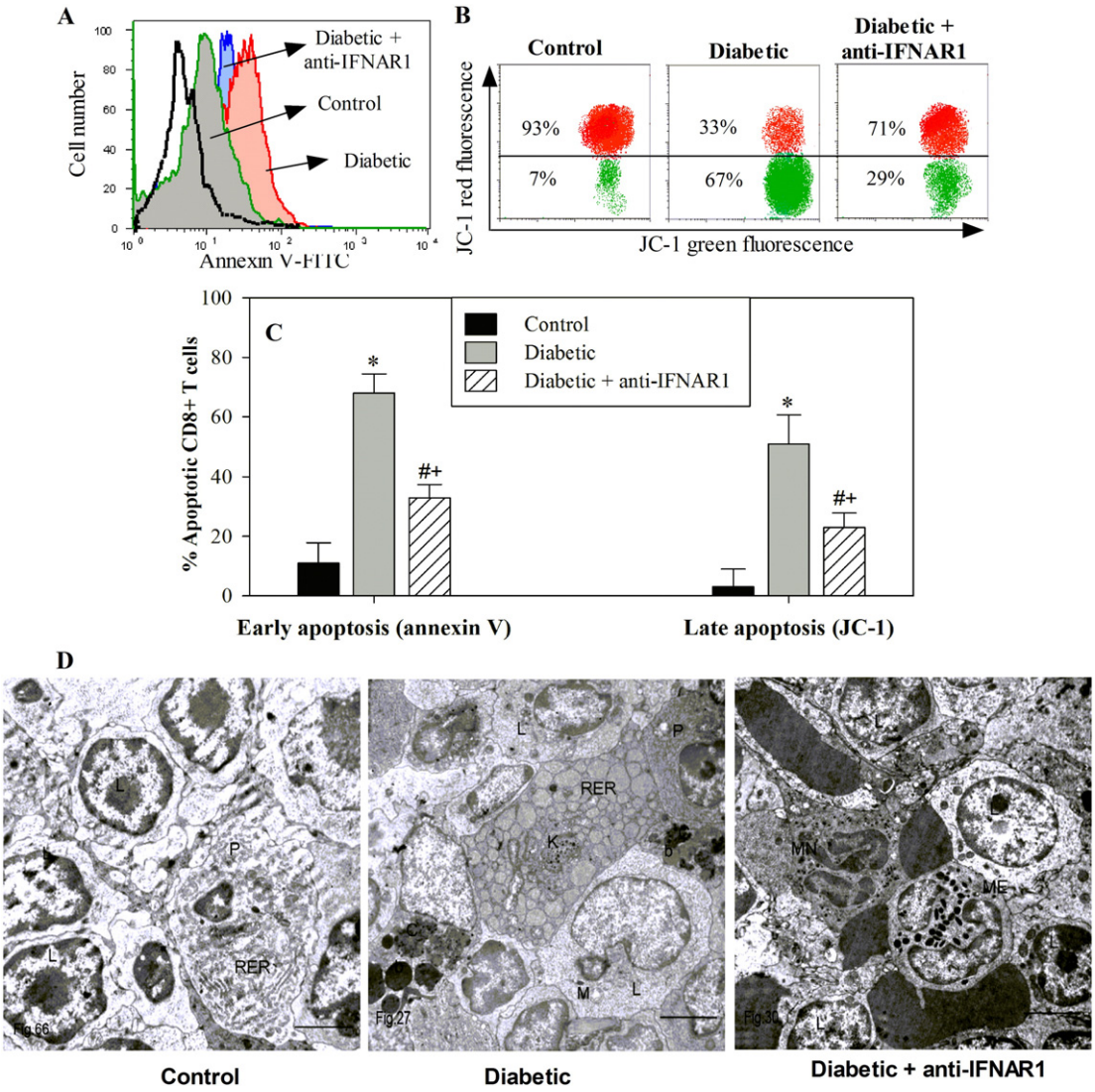

Fig. 3. Increased apoptosis in the diabetic mouse spleen CD8 + T cells. The potential for the increased IFN-α, which was observed during diabetes, to induce early apoptosis of CD8 + T cells was determined with flow cytometry, based on Annexin V staining patterns. (A) A flow chart of one representative experiment is shown. Changes in the mitochondrial membrane potential were monitored with JC-1 changes and flow cytometry (B). One representative experiment is shown, in which the late apoptotic (lower green-colored dots) and healthy (upper red-colored dots) CD8 + T cells cluster into distinct groups. (C) Accumulated data from 10 experiments are expressed as the mean percentage of both early and late apoptotic cells ± SEM for CD8 + T cells that were isolated from all groups; *P < 0.05, diabetic vs. control; + P < 0.05, diabetic + anti-IFNAR1 vs. control; #P < 0.05, diabetic + anti-IFNAR1 vs. diabetic. (D) Electron micrographs of the spleens from the three animal groups (3600×). One representative experiment out of three is shown.

restored the numbers of healthy mature and immature lymphocytes and decreased the severe apoptotic changes, such as the degenerated lymphocytes.

3.5. IFNAR1 blockade in diabetic mice restores CCR7 surface expression on spleen CD8 + T cells and their responsiveness to CCL21, which in turn, facilitates their entry into splenic tissues

CCL21 and its receptor, CCR7, play essential roles in the trafficking and homing of CD8 + T cells to lymphoid tissues, and especially the spleen. We therefore investigated the surface expression of CCR7 on CD8 + T cells that were isolated from the spleen and their responsiveness to the cognate ligand, CCL21, in the three mouse groups. T cells that were isolated from the spleens of ten mice from each group were double stained with PE-conjugated anti-CD8 and FITC-conjugated anti-CCR7 to monitor the CCR7 surface expression within the CD8 + T cells subpopulation. As shown from one representative experiment, the mean fluorescence intensity (MFI) indicating the CD8 + T cell CCR7 expression of the diabetic mouse (red, filled histogram) was markedly decreased by seven-fold compared with the control non-diabetic mice (green, filled histogram; Fig. 4A). Nevertheless, the diabetic mice that were treated with anti-IFNAR1 (blue, filled histogram) exhibited a partial restoration of their surface CCR7 expression by four-fold on their spleen CD8 + T cells compared with the diabetic non-treated mice. The accumulated data from ten mice per group showed a significant down-regulation of CCR7 expression on splenic CD8 + T cells in the diabetic group (gray, filled bar) compared with the control group (black, filled bar; Fig. 4B). Moreover, blocking type I IFN receptor partially and significantly restored the CCR7 expression in the splenic CD8 + T cells (hatched bar). We next investigated the impact of CCL21-mediated specific migration of splenic CD8 + T cells using a chemotaxis assay and flow cytometry analyses. The percentage of CD8 + T cells that migrated specifically towards CCL21 was significantly decreased in the diabetic group compared with the control group (n = 10; Fig. 4C). Interestingly, the anti-IFNAR1-treated diabetic group exhibited a significant increase in the percentage of CD8 + T cells that migrated towards CCL21 compared with the diabetic non-treated group.

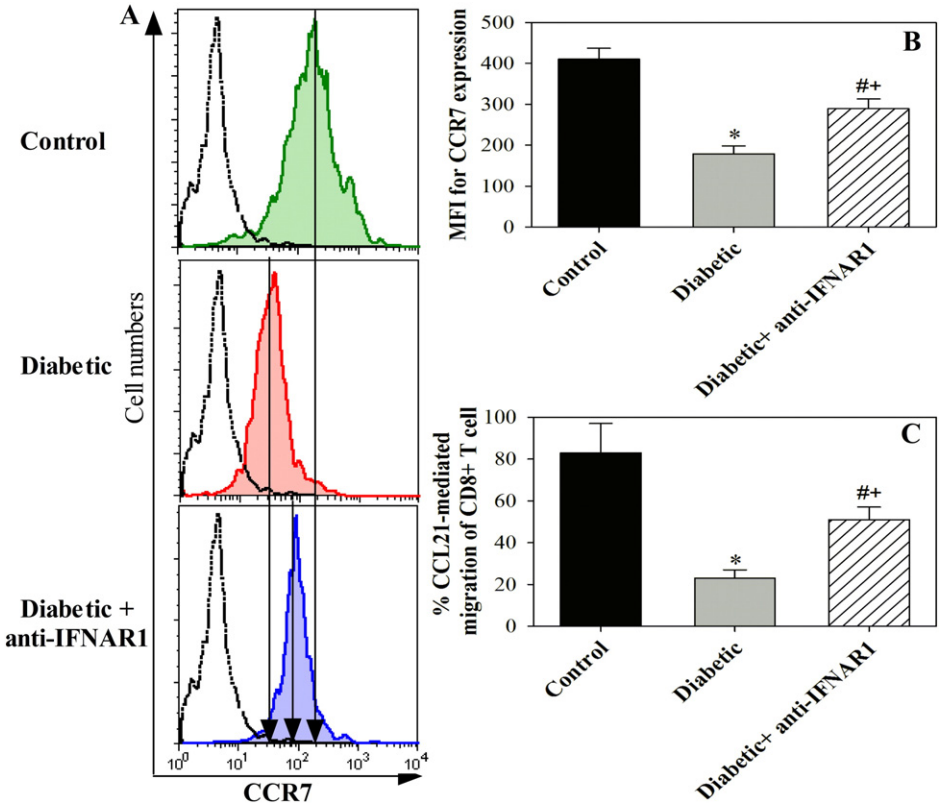

Fig. 4. The effect of type 1 IFN receptor blockade in diabetic mice on spleen CD8 + T cell CCR7 surface expression and their responses to CCL21. CCR7 surface expression was analyzed with flow cytometry. (A) Splenic T cells were isolated from all of the groups and then harvested, cultured overnight at 37 °C in culture medium and washed twice in PBS. The cells were then stained for 30 min at 4 °C with PE-conjugated CD8, FITC-conjugated CCR7 and isotype-matched control (IgG) mAbs. The cells were then washed in PBS and fixed in fixation buffer, and the analyzed cell populations were gated on the viable CD8 + T cell subpopulation. (B) The accumulated CCR7 expression data from 10 experiments from each group are expressed as the mean ± SEM. The chemokine-dependent migration of splenic CD8 + T cells was measured with an in vitro transwell chemotaxis assay followed by flow cytometry analysis. All chemotaxis assays were performed in pre-warmed migration buffer alone or CCL21-supplemented buffer. (C) Accumulated results from all of the groups (10 mice/group) are expressed as the mean number of migrated cells ± SEM; *P < 0.05, diabetic vs. control; +P < 0.05, diabetic + anti-IFNAR1 vs. control; #P < 0.05, diabetic + anti-IFNAR1 vs. diabetic.

3.6. IFNAR1 blockade in diabetic mice enhances CD127 surface expression on spleen CD8 + T cells and restores IL-7-mediated STAT5 and AKT phosphorylation

IL-7, through its receptor CD127 (IL-7 receptor α), induces proliferation and sustains long-lived memory CD8 + T cells. As we previously detected a marked decrease in the IL-7 levels in diabetic mice compared with control non-diabetic animals, we investigated the CD127 surface expression on CD8 + T cells isolated from the spleens of the three animal groups. T cells were isolated from the spleens of ten mice from each group and then double stained with PE-conjugated anti-CD8 and FITC-conjugated anti-CD127 to monitor the CD127 surface expression within the CD8 + T cell subpopulation using flow cytometry analysis. Our results showed a significant decrease in the CD127 surface expression MFI on the splenic CD8 + T cells of the diabetic mice (gray, filled bar) compared with the control non-diabetic mice (black, filled bar; Fig. 5A). By contrast, the anti-IFNAR1 Ab-treated diabetic mice (hatched bar) exhibited a significant restoration in the CD127 expression on their CD8 + T cells compared with the diabetic non-treated mice.

To determine whether the signaling pathways downstream of CD127, which are known to sustain survival and rescue CD8 + T cells from apoptosis, were perturbed in diabetic mice, splenic CD8 + T cells were stimulated or not with IL-7 for 5 min. Cell lysates were prepared for Western blot analysis to investigate STAT5 and AKT phosphorylation and expression levels. Immunoblots from one representative experiment of ten independent experiments are shown (Fig. 5B) for the AKT and STAT5 phosphorylation analyses. Total AKT and STAT5 levels were used as equal loading controls. We clearly observed that the diabetic mice exhibited a marked reduction in the IL-7-mediated STAT5 and AKT phosphorylation in splenic CD8 + T cells compared with the control non-diabetic mice. Furthermore, type 1 IFN signaling blockade in the diabetic mice partially restored the IL-7-mediated STAT5 and AKT phosphorylation in the splenic CD8 + T cells. The data acquired from ten animals per group were analyzed and expressed as the normalized average of the phosphorylated protein to the total relevant protein ± SEM (Fig. 5C). In this context, IL-7 stimulation of the splenic CD8 + T cells isolated from the control non-diabetic group resulted in a marked phosphorylation of AKT and STAT5 compared with those in the cells that were left unstimulated. By contrast, a significant reduction in the AKT and STAT5 phosphorylation was observed in the diabetic group upon IL-7 stimulation compared with the control non-diabetic group. Type I IFN receptor blockade in the diabetic mice partially and significantly restored the AKT and STAT5 phosphorylation levels upon IL-7 stimulation. However, if we subtracted the normalized phosphorylation levels of these proteins without stimulation from their values upon IL-7 stimulation, this calculation revealed that the CD8 + T cells that were isolated from the diabetic group had significantly perturbed AKT and STAT5 phosphorylation levels upon IL-7 stimulation, which subsequently makes these cells more susceptible to elimination by apoptosis.

4. Discussion

T1D is an insulin-dependent autoimmune disease that is characterized by the loss of 80% of insulin-producing cells [43]. Different mechanisms lead to pancreatic islet β-cell apoptosis in T1D [44]. IFN-α is a group of pleiotropic cytokines in the type I family of IFNs [45]. The type 1 IFNs are potent pro-inflammatory cytokines that can be

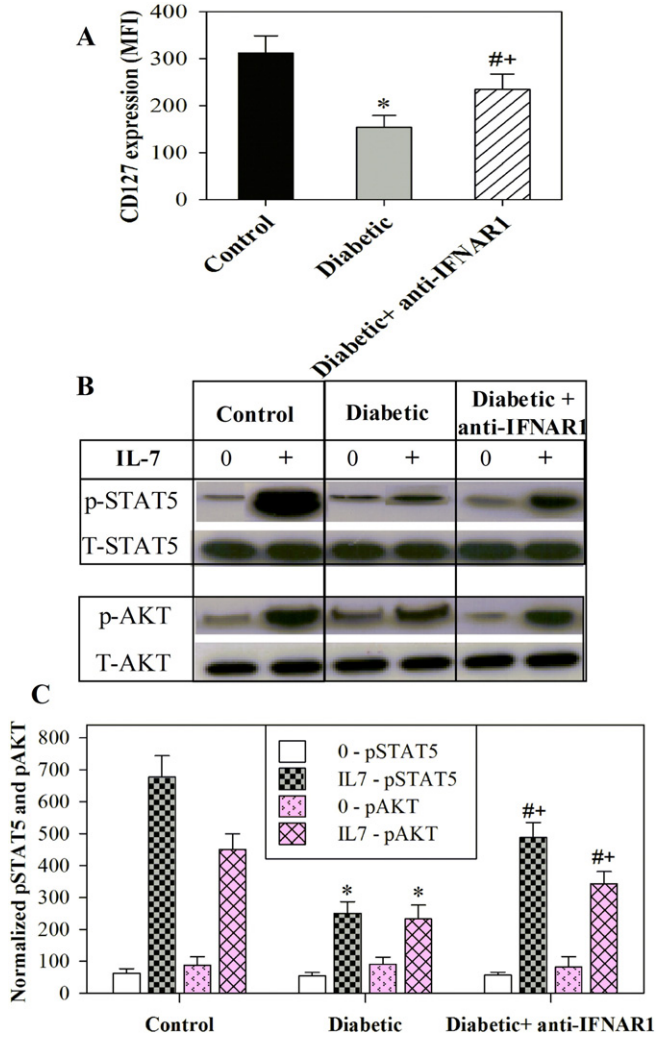

Fig. 5. Splenic CD8 + T cells from diabetic mice exhibit decreased CD127 expression and downstream signaling perturbation. CD127 surface expression on splenic CD8 + T cells that were isolated from all of the groups was analyzed with flow cytometry. (A) Accumulated CD127 MFI results from each group are expressed as the mean ± SEM. The spleen T cell population was isolated from ten mice per group and was stimulated or not with IL-7 for 5 min. Cell lysates were then prepared for Western blot analysis. Immunoblots from representative experiments are shown for the AKT and STAT5 expression and phosphorylation levels (B). The data acquired for ten individual mice per group are expressed as the normalized average of the phosphorylated protein to the total relevant protein levels ± SEM, as shown in (C). For the unstimulated vs. IL-7-stimulated cells, the normalized phosphoprotein level values in the unstimulated cells were subtracted from those in the IL-7-stimulated cells to yield the specific phosphorylation values. The statistical analysis of the specific phosphorylation values revealed that *$P < 0.05$, diabetic vs. control; +$P < 0.05$, diabetic + anti-IFNAR1 vs. control; #$P < 0.05$, diabetic + anti-IFNAR1 vs. diabetic.

generated by most if not all cell types. Additionally, IFN-α has intensified effects on innate and adoptive immune responses [46]. Many previous studies have suggested the involvement of IFN-α in the development of T1D. Several studies have shown elevated IFN-α mRNA and protein levels in the pancreata of T1D patients compared with non-diabetic patients [47,48]. Therefore, studying the role of IFN-α in T1D pathogenesis is of high significance [49]. In our recent study, we demonstrated that blocking type 1 IFN signaling in diabetic mice significantly returned the insulin and lipid profiles to normal levels, which subsequently restored the B cell distribution and rescued peripheral B cells from cell death [50]. In the present study, we investigated the effect of type 1 IFN receptor blockade on spleen-homing CD8 + T cells in a streptozotocin-induced type 1 diabetic mouse model. As shown in previous diabetic mouse model studies, the loss of the insulin-producing β cells of the pancreas caused elevated glucose levels in correlation with decreased insulin levels [51]. Up-regulation in type 1 IFN is a prominent feature of T1D [52], which consequently leads to exhaustion of lymphoid organ-homing T lymphocytes [53]. Li and colleagues identified the up-regulation of a number of genes in CD4 + T cells that were purified from PLNs as a result of IFN-α elevation [54]. Oxidative stress has a significant role in T1D development [55]. Increased oxidative stress has emerged as playing a central role in the initiation and progression of many autoimmune diseases [56–58]. Therefore, several studies have provided evidences for successful use of natural antioxidants in the prevention and treatment of the oxidative stress-mediating immune complications [59–61]. Therefore, diabetes is accompanied by high free radical levels in the blood and spleen (Fig. 1). Furthermore, increased ROS levels stimulate inflammatory cytokine production, primarily IL-6, which is considered the primary regulator of the acute inflammatory response. However, all inflammatory cytokines exhibit cytotoxic and cytostatic activities and have the ability to induce apoptosis in pancreatic islet cells [62,63]. It has been established that TNF-α plays multiple roles in the development and function of the immune system. TNF-α promotes the up-regulation of adhesion molecules and activation of macrophages, and it is necessary for T1D development in NOD mice [64]. Although IL-6 and TNF-α are significantly increased in diabetic model, IL-7 is highly decreased; therefore, a significant decrease in the number of spleen-homing CD8 + T cells was observed. Chemokines play a crucial role in immune cell chemotaxis. Particularly, CCL21 participates in naive T and B cell recruitment to the extra-follicular area in secondary lymphoid organs [65]. Previous studies have determined the key role of CCL21 and its lymphocyte receptor (CCR7) in the migration of lymphocytes from the blood into lymphoid tissues, especially the spleen [66–68]. The present flow cytometric analysis of the CCR7 and CCL21 surface expression of splenic CD8 + T cells confirmed the above-mentioned role of CCR7/CCL21. In the present study, splenic CD8 + T cells isolated form the diabetic mice exhibited marked elevation in apoptosis induction and an obvious reduction in CCL21-mediated their entry to the spleen, suggesting that both these two mechanisms contribute to the exhaustion state and depletion of CD8 + T cells from the spleen of diabetic animals.

IL-7 is a crucial cytokine for the development and homeostatic maintenance of T and B lymphocytes [69]. Meanwhile, IL-7 suppresses apoptosis through the up-regulation of the anti-apoptotic protein BCL-2 and the down-regulation of the pro-apoptotic protein Bax [70,71]. We previously demonstrated that early interferon therapy for hepatitis C virus infection rescues polyfunctional, long-lived CD8 + memory T cells through IL-7/CD127 dependent mechanisms [72]. Therefore our results demonstrate that decreased IL-7 level, CD127 expression or downstream signaling affect the survival and functions of memory CD8 + T cells and render the diabetic individuals more susceptible to infection. It has also been established that IL-7 plays complimentary or overlapping roles in maintaining CD8 + T cells after antigen stimulation [73]. CD8 + T-cell survival may be impaired in the absence of IL-7 [32]. Reduced CD127 expression on CD8 + T cells of diabetic animals may contribute to the observed decline in T cell functions associated with diabetes by affecting the ability of these cells to respond to IL-7. Alternatively, disease-associated defects of T cells may also influence IL-7 responsiveness of cells that express CD127. In support of this, it was shown that effector CD8 + T cells destined to become long-lived memory cells selectively express CD127, suggesting that these cells might be preferentially IL-7 dependent [35]. In addition, it was found that acute homeostatic proliferation of memory CD8 + T cells displayed overlapping dependency on endogenous IL-7 [74]. Our results are in agreement with previous study reported that CD127 down-regulation on CD8 + T cells during HIV infection may contribute to the observed impairment in CTL activity and IL-7 production which thought to be attempt to counteract lymphopenia [75]. Despite decrease in IL-7, CD8 + T cells response becomes progressively impaired within diabetes, suggesting

an inability of CD8 + T cells to respond to IL-7. Impaired CD8 + T cell function and decreased CD127 expression have recently been linked to abnormal activation of the immune system and are contributed to immunodeficiency [76]. A recent study confirmed that removing CD127 (IL-7R α) from the cell surface leads to an HIV Tat protein mediated-reduction of IL-7 signaling and impairs CD8 T cell proliferation and function [77], which we similarly observed, as shown in Figs. 4 and 5A. Moreover, IL-7 signaling depends primarily on the engagement of CD127 and the common gamma chain on the T cell surface, which phosphorylates STAT5 and AKT [78,79]. Furthermore, STAT5 activation strongly enhances effector and memory CD8 T cell survival and homeostatic proliferation, AKT activation, and BCL2 expression [79]. IL-7/IL-7R signaling reportedly initiates at least two separate signaling cascades, the Jak/STAT pathway and the phosphatidylinositol-3 (PI3) kinase/Akt pathway [80]. Each of these cascades is thought to separately regulate Bcl-2 family members to promote survival of activated cells and increase resistance to apoptosis [81,82]. The data presented here address the additional explanation that reduced IL-7 level and activity during diabetes is not only a result of a decrease in CD127 expression but may also be a result of defects in CD127 signaling. As IL-7 has been reported to drive T cell proliferation via STAT5 [83], impairment of CD8 + T cells from diabetic animals (Fig. 6) in response to IL-7 may be a result of diminished IL-7's ability to phosphorylate STAT5 and may be a mechanism contributing to the CD8 + T cell impairment. While it has been demonstrated in other disease states that IL-7 stimulation failed to activate STAT5 in a significant proportion of CD8 + T cells suggested that impaired IL-7/IL-7R signaling is associated with defects in CD8 + T cell responses [84]. In this context, it has been established that the activation of STAT5 through JAK3 has been implicated in IL-7-dependent synthesis of Bcl-2 [83]. The production of Bcl-2 in response to IL-7 has been shown recently to depend on the Jak/STAT5 pathway [48], therefore the present data suggest that the defect observed in diabetic animals may be limited to this pathway. In addition, this observation may be explained by findings by Barata et al. [85], where PI3K activation was shown to be required for IL-7-mediated Bcl-2 up-regulation in a leukemic T cell line, suggesting that, in addition to STAT5, other molecules are required and that phosphorylation of STAT5 may not be the limiting process. While, it was reported that activation of STAT5 independently initiates cell cycle progression or PI3K pathway [86], our observation of impairment of AKT phosphorylation upon IL-7 stimulation during diabetes proved an additional mechanism contributing to the CD8 + T cell impairment observed in type 1 diabetes that may be an altered ability to acquire sufficient nutrients to support cellular metabolism. Several studies demonstrated that IL-7 maintains metabolic activity through the uptake of glucose from the extracellular milieu [83,87]. Furthermore, IL-7-mediated PI3K/AKT signaling results in the regulation of expression and activity of the glucose transporter GLU1 and the transferin receptor CD71, which are important in the control of cell growth [85]. In conclusion, we proved in this study that beside the additional effect of down-regulating CD127 expression, an alternative explanation for CD8 + T cell dysfunction is impairment in IL-7-mediated signaling via impairment in the phosphorylation of STAT5 and AKT which would impede the biological function of IL-7 on CD8 + T cells during diabetes.

5. Conclusions

Taken together, our results explain the increased apoptosis of CD8 + T cells through the reduction of IL-7-mediated STAT5 and AKT activation. Remarkably, type 1 IFN blockade in diabetic mice significantly restored free radical and pro-inflammatory cytokine levels. Additionally, IL-7 and its receptor, CD127, were restored, which in turn rescued CD8 + T cells from apoptosis. Thus, our data suggest that type 1 IFN is a crucial regulator of spleen-homing CD8 + T cells during T1D development.

Conflict of interests

The authors declare no conflicts of interest. This manuscript has not been published or submitted elsewhere. This work complies with the Ethical Policies of this Journal and has been conducted under internationally accepted ethical standards after relevant ethical review. All authors have approved the final article.

Acknowledgments

The authors would like to extend their sincere appreciation to the Deanship of Scientific Research at King Saud University for its funding of this Research group NO (**RG-1435-019**).

References

[1] K. Kelemen, Adv. Exp. Med. Biol. 552 (2004) 117–128.
[2] A. Zoka, G. Barna, A. Somogyi, G. Muzes, A. Olah, Z. Al-Aissa, O. Hadarits, K. Kiss, G. Firneisz, Autoimmunity (2014) 1–9, http://dx.doi.org/10.3109/08916934.2014.992518.
[3] M. Cnop, N. Welsh, J.C. Jonas, A. Jorns, S. Lenzen, D.L. Eizirik, Diabetes 54 (Suppl. 2) (2005) S97–S107.
[4] D.L. Eizirik, T. Mandrup-Poulsen, Diabetologia 44 (2001) 2115–2133.
[5] M.S. Anderson, J.A. Bluestone, Annu. Rev. Immunol. 23 (2005) 447–485.
[6] D.A. Gutierrez, W. Fu, S. Schonefeldt, T.B. Feyerabend, A. Ortiz-Lopez, Y. Lampi, A. Liston, D. Mathis, H.R. Rodewald, Diabetes 63 (2014) 3827–3834.
[7] K. Haskins, Adv. Immunol. 87 (2005) 123–162.
[8] S. Pestka, Biopolymers 55 (2000) 254–287.
[9] C.A. Biron, Immunity 14 (2001) 661–664.
[10] A.N. Theofilopoulos, R. Baccala, B. Beutler, D.H. Kono, Annu. Rev. Immunol. 23 (2005) 307–336.
[11] N. Hata, M. Sato, A. Takaoka, M. Asagiri, N. Tanaka, T. Taniguchi, Biochem. Biophys. Res. Commun. 285 (2001) 518–525.
[12] H.M. Ibrahim, I.A. El-Elaimy, H.M. Saad Eldien, B.M. Badr, D.M. Rabah, G. Badr, Oxidative Med. Cell. Longev. 2013 (2013) 148725.
[13] R. Otton, J.R. Mendonca, R. Curi, J. Endocrinol. 174 (2002) 55–61.
[14] V.B. Shidham, V.K. Swami, Arch. Pathol. Lab. Med. 124 (2000) 1291–1294.
[15] X. Huang, J. Yuang, A. Goddard, A. Foulis, R.F. James, A. Lernmark, R. Pujol-Borrell, A. Rabinovitch, N. Somoza, T.A. Stewart, Diabetes 44 (1995) 658–664.
[16] C. Le Page, P. Genin, M.G. Baines, J. Hiscott, Rev. Immunogenet. 2 (2000) 374–386.
[17] C. Pimson, W. Chatuphonprasert, K. Jarukamjorn, Pak. J. Pharm. Sci. 27 (2014) 1731–1737.
[18] S. Golbidi, M. Badran, I. Laher, Exp. Diabetes Res. 2012 (2012) 941868.
[19] M.P. Francescato, G. Stel, M. Geat, S. Cauci, PLoS One 9 (2014) e99062.
[20] K. Alexandraki, C. Piperi, C. Kalofoutis, J. Singh, A. Alaveras, A. Kalofoutis, Ann. N. Y. Acad. Sci. 1084 (2006) 89–117.
[21] J.G. Cyster, Science 286 (1999) 2098–2102.
[22] K.T. Coppieters, F. Dotta, N. Amirian, P.D. Campbell, T.W. Kay, M.A. Atkinson, B.O. Roep, M.G. von Herrath, J. Exp. Med. 209 (2012) 51–60.
[23] L.S. Wicker, E.H. Leiter, J.A. Todd, R.J. Renjilian, E. Peterson, P.A. Fischer, P.L. Podolin, M. Zijlstra, R. Jaenisch, L.B. Peterson, Diabetes 43 (1994) 500–504.
[24] D.V. Serreze, H.D. Chapman, D.S. Varnum, I. Gerling, E.H. Leiter, L.D. Shultz, J. Immunol. 158 (1997) 3978–3986.
[25] B. Anderson, B.J. Park, J. Verdaguer, A. Amrani, P. Santamaria, Proc. Natl. Acad. Sci. U. S. A. 96 (1999) 9311–9316.
[26] K.M. Ansel, L.J. McHeyzer-Williams, V.N. Ngo, M.G. McHeyzer-Williams, J.G. Cyster, J. Exp. Med. 190 (1999) 1123–1134.
[27] M.D. Gunn, S. Kyuwa, C. Tam, T. Kakiuchi, A. Matsuzawa, L.T. Williams, H. Nakano, J. Exp. Med. 189 (1999) 451–460.
[28] V.N. Ngo, H.L. Tang, J.G. Cyster, J. Exp. Med. 188 (1998) 181–191.
[29] R. Forster, A. Schubel, D. Breitfeld, E. Kremmer, I. Renner-Muller, E. Wolf, M. Lipp, Cell 99 (1999) 23–33.
[30] Z. Shan, B. Xu, A. Mikulowska-Mennis, S.A. Michie, Immunol. Res. 58 (2014) 351–357.
[31] C. Potsch, D. Vohringer, H. Pircher, Eur. J. Immunol. 29 (1999) 3562–3570.
[32] K.S. Schluns, W.C. Kieper, S.C. Jameson, L. Lefrancois, Nat. Immunol. 1 (2000) 426–432.
[33] Y. Okamoto, D.C. Douek, R.D. McFarland, R.A. Koup, Blood 99 (2002) 2851–2858.
[34] T.J. Fry, C.L. Mackall, Blood 99 (2002) 3892–3904.
[35] S.M. Kaech, J.T. Tan, E.J. Wherry, B.T. Konieczny, C.D. Surh, R. Ahmed, Nat. Immunol. 4 (2003) 1191–1198.
[36] J.H. Park, Q. Yu, B. Erman, J.S. Appelbaum, D. Montoya-Durango, H.L. Grimes, A. Singer, Immunity 21 (2004) 289–302.
[37] S. Beq, J.F. Delfraissy, J. Theze, Eur. Cytokine Netw. 15 (2004) 279–289.
[38] L.F. Lee, K. Logronio, G.H. Tu, W. Zhai, I. Ni, L. Mei, J. Dilley, J. Yu, A. Rajpal, C. Brown, C. Appah, S.M. Chin, B. Han, T. Affolter, J.C. Lin, Proc. Natl. Acad. Sci. U. S. A. 109 (2012) 12674–12679.
[39] G. Badr, H. Waly, H.M. Eldien, H. Abdel-Tawab, K. Hassan, I.M. Alhazza, H. Ebaid, S.H. Alwasel, Cell. Physiol. Biochem. 26 (2010) 1029–1040.
[40] G. Badr, Lipids Health Dis. 12 (2013) 46.
[41] G. Badr, M.K. Al-Sadoon, D.M. Rabah, D. Sayed, Apoptosis 18 (2013) 300–314.

[42] J.I. Odegaard, A. Chawla, Cold Spring Harb. Perspect. Med. 2 (2012) a007724.
[43] J.A. Wali, P. Trivedi, T.W. Kay, H.E. Thomas, Methods Mol. Biol. 1292 (2015) 165–176.
[44] F.P. Siegal, N. Kadowaki, M. Shodell, P.A. Fitzgerald-Bocarsly, K. Shah, S. Ho, S. Antonenko, Y.J. Liu, Science 284 (1999) 1835–1837.
[45] K.B. Nguyen, L.P. Cousens, L.A. Doughty, G.C. Pien, J.E. Durbin, C.A. Biron, Nat. Immunol. 1 (2000) 70–76.
[46] A. Rabinovitch, Diabetes Metab. Res. Rev. 14 (1998) 129–151.
[47] A.K. Foulis, M.A. Farquharson, A. Meager, Lancet 2 (1987) 1423–1427.
[48] Q. Li, B. Xu, S.A. Michie, K.H. Rubins, R.D. Schreriber, H.O. McDevitt, Proc. Natl. Acad. Sci. U. S. A. 105 (2008) 12439–12444.
[49] B.M. Badr, N.A. Moustafa, H.M. Eldien, A.O. Mohamed, H.M. Ibrahim, I.A. El-Elaimy, M.H. Mahmoud, G. Badr, Cell. Physiol. Biochem. 35 (2015) 137–147.
[50] Tom L. Van Belle, Ken T. Coppieters, M.G.V. Herrath, Physiol. Rev. 91 (2011) 79–118.
[51] L. Yip, C.G. Fathman, Immunol. Res. 58 (2014) (2014) 340–350.
[52] R. Ou, S. Zhou, L. Huang, D. Moskophidis, J. Virol. 75 (2001) 8407–8423.
[53] S. Trembleau, G. Penna, S. Gregori, N. Giarratana, L. Adorini, J. Immunol. 170 (2003) 5491–5501.
[54] R. Bottino, A.N. Balamurugan, H. Tse, C. Thirunavukkarasu, X. Ge, J. Profozich, M. Milton, A. Ziegenfuss, M. Trucco, J.D. Piganelli, Diabetes 53 (2004) 2559–2568.
[55] G. Badr, B.M. Badr, M.H. Mahmoud, M. Mohany, D.M. Rabah, O. Garraud, BMC Immunol. 13 (2012) 32.
[56] G. Badr, H. Ebaid, M. Mohany, A.S. Abuelsaad, J. Nutr. Biochem. 23 (2012) 1640–1646.
[57] G. Badr, M.K. Al-Sadoon, A.M. El-Toni, M. Daghestani, Lipids Health Dis. 11 (2012) 27.
[58] G. Badr, O. Garraud, M. Daghestani, M.S. Al-Khalifa, Y. Richard, Cell. Immunol. 273 (2012) 10–16.
[59] G. Badr, M. Mohany, F. Abu-Tarboush, Lipids Health Dis. 10 (2011) 236.
[60] G. Badr, S. Alwasel, H. Ebaid, M. Mohany, I. Alhazza, Cell. Immunol. 267 (2011) 133–140.
[61] J.S. Reis, C.A. Amaral, C.M. Volpe, J.S. Fernandes, E.A. Borges, C.A. Isoni, P.M. Anjos, J.A. Machado, Arq. Bras. Endocrinol. Metabol. 56 (2012) 441–448.
[62] M. Brownlee, Diabetes 54 (2005) 1615–1625.
[63] L.F. Lee, B. Xu, S.A. Michie, G.F. Beilhack, T. Warganich, S. Turley, H.O. McDevitt, Proc. Natl. Acad. Sci. U. S. A. 102 (2005) 15995–16000.
[64] T. Junt, E. Scandella, R. Forster, P. Krebs, S. Krautwald, M. Lipp, H. Hengartner, B. Ludewig, J. Immunol. 173 (2004) 6684–6693.
[65] C. Ploix, D. Lo, M.J. Carson, J. Immunol. 167 (2001) 6724–6730.
[66] G. Badr, M. Mohany, A. Metwalli, Lipids Health Dis. 10 (2011) 203.
[67] S. Mori, H. Nakano, K. Aritomi, C.R. Wang, M.D. Gunn, T. Kakiuchi, J. Exp. Med. 193 (2001) 207–218.
[68] M.J. Palmer, V.S. Mahajan, L.C. Trajman, D.J. Irvine, D.A. Lauffenburger, J. Chen, Cell. Mol. Immunol. 5 (2008) 79–89.
[69] J. Gao, L. Zhao, Y.Y. Wan, B. Zhu, Int. J. Mol. Sci. 16 (2015) 10267–10280.
[70] L. Lu, P. Chaudhury, D.G. Osmond, J. Immunol. 162 (1999) 1931–1940.
[71] E.M. Faller, S.M. Sugden, M.J. McVey, J.A. Kakal, P.A. MacPherson, J. Immunol. 185 (2010) 2854–2866.
[72] G. Badr, N. Bédard, M.S. Abdel-Hakeem, L. Trautmann, B. Willems, J.P. Villeneuve, E.K. Haddad, R.P. Sékaly, J. Bruneau, N.H. Shoukry, J. Virol. 82 (20) (Oct. 2008) 10017–10031.
[73] S.C. Jameson, Semin. Immunol. 17 (2005) 231–237.
[74] J.T. Tan, B. Ernst, W.C. Kieper, E. LeRoy, J. Sprent, C.D. Surh, J. Exp. Med. 195 (2002) 1523–1532.
[75] L.A. Napolitano, R.M. Grant, S.G. Deeks, D. Schmidt, SC,m De Rosa, L.A. Herzenberg, B.G. Herndier, J. Andersson, J.M. McCune, Nat. Med. 7 (2001) 73–79.
[76] J.H. Colle, J.L. Moreau, A. Fontanet, O. Lambotte, M. Joussemet, S. Jacod, J.F. Delfraissy, J. Theze, J. Acquir. Immune Defic. Syndr. 42 (2006) 277–285.
[77] C. Pallard, A.P. Stegmann, T. van Kleffens, F. Smart, A. Venkitaraman, H. Spits, Immunity 10 (1999) 525–535.
[78] P. Monti, C. Brigatti, M. Krasmann, A.G. Ziegler, E. Bonifacio, Diabetes 62 (2013) 2500–2508.
[79] T.W. Hand, W. Cui, Y.W. Jung, E. Sefik, N.S. Joshi, A. Chandele, Y. Liu, S.M. Kaech, Proc. Natl. Acad. Sci. U. S. A. 107 (2010) 16601–16606.
[80] R. Hofmeister, A.R. Khaled, N. Benbernou, E. Rajnavolgyi, K. Muegge, S.K. Durum, Cytokine Growth Factor Rev. 10 (1999) 41–60.
[81] C.L. Amos, A. Woetmann, M. Nielsen, C. Geisler, N. Odum, B.L. Brown, P.R. Dobson, Cytokine 10 (1998) 662–668.
[82] Q. Jiang, W.Q. Li, R.R. Hofmeister, H.A. Young, D.R. Hodge, J.R. Keller, A.R. Khaled, S.K. Durum, Mol. Cell. Biol. 24 (2004) 6501–6513.
[83] J.A. Wofford, H.L. Wieman, S.R. Jacobs, Y. Zhao, J.C. Rathmell, Blood 111 (2008) 2101–2111.
[84] A. Benoit, K. Abdkader, D. Sirskyj, A. Alhetheel, N. Sant, J.B. Angel, A. Kumar, F. Diaz-Mitoma, M. Kryworuchko, 4th IAS Conference, on HIV Pathogenesis, Treatment and Prevention, Sydney, Australia, 2004.
[85] J.T. Barata, A. Silva, J.G. Brandao, L.M. Nadler, A.A. Cardoso, V.A. Boussiotis, J. Exp. Med. 200 (2004) 659–669.
[86] L. Swainson, S. Kinet, C. Mongellaz, M. Sourisseau, T. Henriques, N. Taylor, Blood 109 (2007) 1034–1042.
[87] A.R. Khaled, D.V. Bulavin, C. Kittipatarin, W.Q. Li, M. Alvarez, K. Kim, H.A. Young, A.J. Fornace, S.K. Durum, J. Cell Biol. 169 (2005) 755–763.